

Non-Abelian Yang-Mills–Higgs vortices

Francisco Navarro-Lérida[‡] and D. H. Tchrakian^{*†}

[‡]Dept.de Física Atómica, Molecular y Nuclear, Universidad Complutense de Madrid, E-28040 Madrid, Spain

^{*}School of Theoretical Physics, Dublin Institute for Advanced Studies, 10 Burlington Road, Dublin 4, Ireland

[†]Department of Computer Science, National University of Ireland Maynooth, Maynooth, Ireland

(Dated: November 5, 2018)

In this Letter we present new, genuinely non-Abelian vortex solutions in $SU(2)$ Yang-Mills–Higgs theory with only one *isovector* scalar field. These non-Abelian solutions branch off their Abelian counterparts (Abrikosov–Nielsen–Olesen vortices) for precise values of the Higgs potential coupling constant λ . For all values of λ , their energies lie below those of the Abelian energy profiles, the latter being logarithmically divergent as $\lambda \rightarrow \infty$. The non-Abelian branches plateau in the limit $\lambda \rightarrow \infty$ and their number increases with λ , this number becoming infinite. For each vorticity, the gaps between the plateauing energy levels become constant. In this limit the non-Abelian vortices are non-interacting and are described by the *self-dual* vortices of the $O(3)$ sigma model. In the absence of a topological lower bound, we expect these non-Abelian vortices to be *sphalerons*.

PACS numbers: 11.15.-q, 11.10.Kk, 11.15.Kc

Introduction

Non-Abelian vortices on \mathbb{R}^2 have attracted interest since a very long time. Nambu [1] pointed out that vortices of finite length in \mathbb{R}^3 require monopoles at each end. Originally, they were proposed by Mandelstam [1] as flux tubes absorbed by non-Abelian ('t Hooft–Polyakov) monopoles at each end. In this picture the monopoles are bound, implying that in the dual picture where the duals of the monopoles are the quarks, one can describe confinement in QCD.

The 't Hooft–Polyakov monopole is a topologically stable and finite energy solution of the $SU(2)$ Yang-Mills–Higgs (YMH) system on \mathbb{R}^3 , where the Higgs field takes its values in the algebra, *i.e.*, that it is an *isovector*, $\vec{\phi} = (\phi^1, \phi^2, \phi^3)$, under $SO(3)$ rotations. Topologically stable and finite energy vortex solutions of the gauged Higgs system on \mathbb{R}^2 on the other hand are supported by the Abelian Higgs model, where the Higgs field is a complex scalar, $\varphi = \phi^1 + i\phi^2$, *i.e.*, it is an *isovector* $\phi^M = (\phi^1, \phi^2)$ under $SO(2)$ rotations. This is the Abrikosov–Nielsen–Olesen (ANO) vortex [2]. The field multiplets in the two models do not match.

To construct a non-Abelian vortex on \mathbb{R}^2 , it was realised by Nielsen and Olesen that it is necessary to have a model with more than one Higgs field. They chose [2] two $SO(3)$ *isovector* Higgs fields, each with its own symmetry breaking potential and vacuum expectation value (VEV), but with the vacuum value of each oriented at different directions in isospace – in the simplest case being orthogonal to each other. In this way the $SO(3)$ gauge group is completely broken on the asymptotic circle of \mathbb{R}^2 , which is necessary for topological stability. Subsequently this construction was extended in models featuring N distinct Higgs fields, generalising the $SU(2)$ vortices of [2] to $SU(N)$ in [3–9]. These vortices, described as Z_N vortices, are not genuinely non-Abelian since their flux is restricted to a single direction along the Cartan subalgebra.

More recently, this problem was considered in the con-

text of $\mathcal{N} = 2$ supersymmetric QCD models by Hanay and Tong [10] by Auzzi *et. al.* [11] and by Eto *et. al.* [12]. The salient feature of these models is that they have both gauge and colour symmetries that are broken by the condensate of the scalar fields in such a way that the unbroken subgroup results in orientational zero modes of the string, responsible for non-Abelian flux.

Non-Abelian vortices have been studied intensively in the context of dual confinement in QCD (see the reviews [13] and [14]). In addition to this physical application, they present important examples of cosmic strings [15, 16], relevant to cosmological phase transitions.

In this Letter we have constructed non-Abelian vortices of a $SU(2)$ YMH model with only **one** algebra valued, *i.e.*, isovector, Higgs field. (Non-Abelian vortices in the Weinberg–Salam model were constructed in [17].) This model features exactly the same field multiplets, on \mathbb{R}^2 , as the YMH system supporting the 't Hooft–Polyakov monopole on \mathbb{R}^3 , differing from the two-Higgs models of [2] and those supporting Z_N vortices, and obviously from the SQCD models of [10, 11].

YMH model and non-Abelian Ansatz

Our model on \mathbb{R}^2 is described by the static Hamiltonian

$$\mathcal{H} = -\frac{1}{2} \text{Tr} F_{ij}^2 - \text{Tr} (D_i \Phi)^2 + (4\lambda)^2 \text{Tr} \left(\frac{1}{4} v^2 + \Phi^2 \right)^2, \quad (1)$$

where $\Phi = -\frac{i}{2} \vec{\phi} \cdot \vec{\sigma}$ is the antihermitian isovector Higgs field, and $A_j = -\frac{i}{2} \vec{A}_j \cdot \vec{\sigma}$, j labeling the coordinate on \mathbb{R}^2 , with $\vec{\sigma} = (\sigma^1, \sigma^2, \sigma^3)$, the Pauli matrices. The gauge field is defined by $F_{\mu\nu} = \partial_\mu A_\nu - \partial_\nu A_\mu + [A_\mu, A_\nu]$ and the gauge covariant derivative is given by $D_\mu = \partial_\mu + [A_\mu, \cdot]$. Note that only A_j , the magnetic components of the $SU(2)$ connection $A_\mu = (A_0, A_j)$, appear in Eq. (1), since in the absence of a Chern–Simons term, the electric component of the connection A_0 vanishes, by virtue of the non-Abelian Julia–Zee theorem [18, 19].

The energy of this model is not endowed with a topological lower bound and *a priori* we would not expect the resulting vortices to be topologically stable. But the question of stability is more subtle than this. The (genuinely) non-Abelian vortices we have constructed numerically, present bifurcations from the corresponding Abelian profiles, on plots of their energies *vs.* the Higgs self-interaction coupling constant λ . Remarkably, it turns out that each non-Abelian profile lies below the corresponding Abelian profile for all values of λ and hence cannot be expected to decay into the Abelian vortex with higher energy than it has. Indeed, we show that in the $\lambda \rightarrow \infty$ limit these non-Abelian vortices are described by the (stable) *self-dual* 'instantons' [20] of the $O(3)$ sigma model on \mathbb{R}^2 . However, since these Abelian vortices embedded in the non-Abelian theory at hand are known to be unstable, one cannot expect this feature of the non-Abelian vortices found here to imply stability. Furthermore, the Belavin–Polyakov 'instantons' feature an arbitrary scale, which indicates instability. Thus, we would expect that our non-Abelian vortices are in effect, *sphalerons*. The quantitative stability analysis will be carried out elsewhere.

The radial Ansatz we use is

$$\begin{aligned} \Phi &= v h \frac{\sigma_r^{(n)}}{2i} - v g \frac{\sigma^3}{2i}, \\ A_j &= -\frac{(\varepsilon \hat{x})_j}{r} \left(c \frac{\sigma_r^{(n)}}{2i} - (a+n) \frac{\sigma^3}{2i} \right), \quad j = 1, 2, \end{aligned} \quad (2)$$

where we denote $\sigma_r^{(n)} = \cos n\varphi \sigma^1 + \sin n\varphi \sigma^2$ and $(\varepsilon \hat{x})_j = (\sin \varphi, -\cos \varphi)$. Here $\{a, c, g, h\}$ are functions of r only and the integer n is the vortex number. This Ansatz, previously used to construct non-Abelian Chern-Simons–Higgs vortices [21], is a consistent truncation of the most general Ansatz.

Equations of motion

Subject to the Ansatz Eq. (2), the Euler-Lagrange equations reduce to the following set of non-linear ordinary differential equations,

$$\begin{aligned} -r \left(\frac{a_r}{r} \right)_r &= -v^2 (a h - c g) h, \\ -r \left(\frac{c_r}{r} \right)_r &= v^2 (a h - c g) g, \\ (r h_r)_r &= \frac{1}{r} (a h - c g) a - 8v^2 \lambda^2 r [1 - (h^2 + g^2)] h, \\ -(r g_r)_r &= \frac{1}{r} (a h - c g) c + 8v^2 \lambda^2 r [1 - (h^2 + g^2)] g, \end{aligned} \quad (3)$$

together with the constraint equation

$$v^2 (h g_r - g h_r) - \frac{1}{r^2} (a c_r - c a_r) = 0. \quad (4)$$

The subscript r denotes ordinary differentiation with respect to r . The energy density now reads

$$\begin{aligned} \mathcal{E} &= \frac{1}{4r^2} (a_r^2 + c_r^2) + \frac{1}{4} v^2 \left[(h_r^2 + g_r^2) + \frac{1}{r^2} (a h - c g)^2 + \right. \\ &\quad \left. 4v^2 \lambda^2 [1 - (h^2 + g^2)]^2 \right], \end{aligned} \quad (5)$$

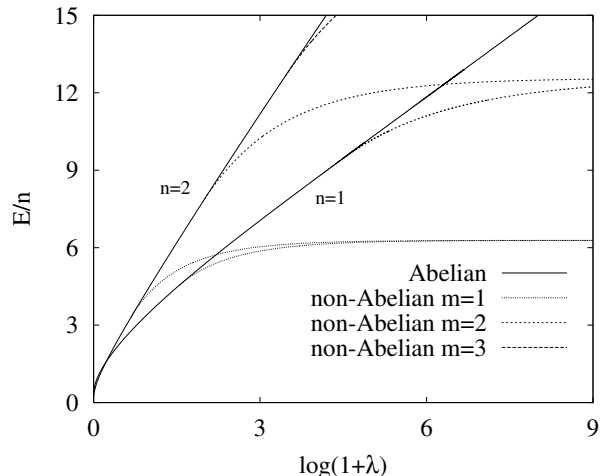


FIG. 1: Energy per vortex number E/n versus the Higgs potential coupling constant λ for YMH solutions with $n = 1, 2$.

the total energy E being given by $E = 2\pi \int r \mathcal{E} dr$.

The embedded Abelian solutions, namely the solutions to the embedded Abelian subsystem, correspond to the truncation $\{c = 0, g = 0\}$. These are the ANO vortices which play an important role in the classification of the non-Abelian vortices we have constructed. In particular we will study the dependence of these on the parameter λ , so it is pertinent at this point to note that the critical configuration of the Abelian vortices corresponds to the value $\lambda = \frac{1}{4}$. This is the Bogomol'nyi limit where the Abelian vortices do not interact.

Numerical results

In order to generate vortex solutions to Eqs. (3)-(4), we impose boundary conditions such that the energy of the solutions is finite and both gauge and the Higgs field functions are regular at the origin. The system of equations is solved numerically by means of a collocation method for boundary-value ordinary differential equations, equipped with an adaptive mesh selection procedure.

The only free parameters are n and λ , since we fixed the unit of length by setting $v = 1$ in what follows. For fixed finite values of these parameters only a finite number of regular solutions exist. There always exists one Abelian solution (ANO solution) for any n and $\lambda (\neq 0)$. For small values of λ this is the only possible solution. However, as λ increases new non-Abelian solutions branch off the Abelian ones. With increasing λ more and more non-Abelian branches appear, their number becoming infinite for $\lambda = \infty$. For given n all the non-Abelian solutions have energy lower than that of their Abelian counterparts for each value of λ . This branch structure of the solutions is exhibited in Fig. 1 where the energy per vortex number, E/n , is plotted versus the constant λ for $n = 1, 2$.

In this figure we observe the first two non-Abelian branches for $n = 1$ and the first three ones for $n = 2$.

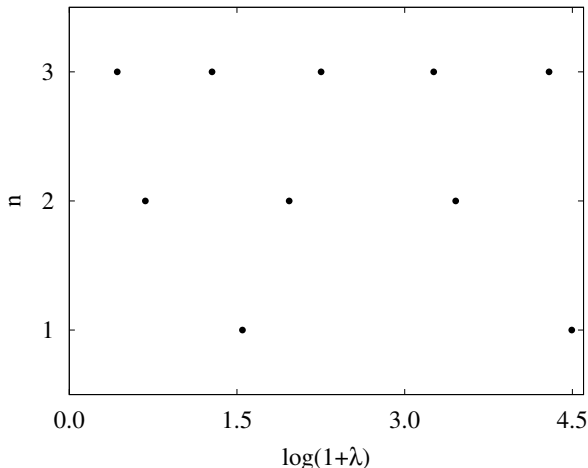


FIG. 2: Location of the first branching points for $n = 1, 2, 3$.

The lowest non-Abelian branch branches off the Abelian solutions at $\lambda \approx 3.705, 0.975$, for $n = 1, 2$, respectively. It is clearly seen that higher values of the vorticity n allow for new non-Abelian branches at lower values of λ . This is more explicitly shown in Fig. 2, where the locations of the first branching points for $n = 1, 2, 3$ are given in logarithmic scale.

The structure of non-Abelian branches may be labeled by the pair (n, m) , n being the vorticity and the integer m indicating the specific non-Abelian branch for that vorticity n (lower m means lower energy). Notice that the Abelian solutions behave in a different way, which we will emphasize below. In fact, although Abelian solutions exist for any non-vanishing value of λ , for each non-Abelian branch there exists a minimal value of λ , $\lambda_{(n,m)}^{\min}$ (which depends on n and m), below which the non-Abelian branch ceases to exist. In fact, at that minimal value the non-Abelian branch matches the corresponding Abelian branch for that value of n , so $\lambda_{(n,m)}^{\min}$ corresponds to the branching points where non-Abelian branches start to exist.

A remarkable fact in Fig. 2 is that the gap between neighbouring branching points is roughly constant for each n on logarithmic scale for λ . More precisely, the quantity $n [\log(1 + \lambda_{(n,m+1)}^{\min}) - \log(1 + \lambda_{(n,m)}^{\min})]$ is roughly constant and independent of (n, m) . This feature becomes more accurate for large λ , revealing an underlying structure in the non-Abelian sector in the limit $\lambda \rightarrow \infty$. In fact, denoting the energy of the (n, m) non-Abelian solutions by $E_{(n,m)} = E_{(n,m)}(\lambda)$, one observes in Fig. 1 that for each m the energy per vortex number tends to a limit which does not depend on n but only on m .

It turns out that

$$\lim_{\lambda \rightarrow \infty} \frac{E_{(n,m)}(\lambda)}{n} = 2\pi m, \quad (6)$$

the energy *per unit* vorticity is equal to the energy of

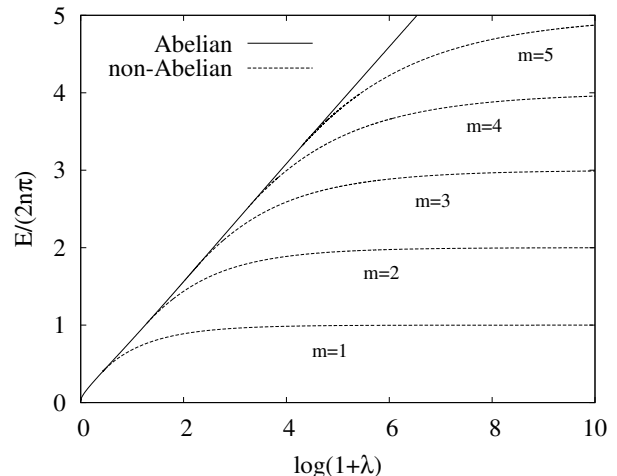


FIG. 3: Energy per vortex number E/n versus the Higgs potential coupling constant λ for YMH solutions with $n = 3$.

the *unit* vortex. Hence non-Abelian vortices with given m are non-interacting in that limit. Fig. 3 shows this limit for $n = 3$ solutions. In that figure it is clearly seen that in the large λ region the ratio $E/(2\pi n)$ approaches the integer value m that labels the non-Abelian branches. One observes an infinite number of non-Abelian branches for each n emerging from the logarithmically divergent Abelian profile, each converging to a finite limit.

One can understand this feature as follows. We have verified that in this limit the contribution of the potential term in Eq. (1) to the energy of the non-Abelian vortices vanishes. (This contrasts with the corresponding situation for the vortices of the Abelian Higgs model.) Thus, the YMH theory supporting the non-Abelian vortices becomes a $O(3)$ sigma model on \mathbb{R}^2 in this limit [26]. Likewise in our case the vanishing of the Higgs potential leads to the $O(3)$ sigma model constraint, resulting in the $SO(3)$ gauged $O(3)$ model, which unlike in the WS case [22], does not satisfy the Derrick scaling requirement for finite energy. To this end, we have verified that in this limit the contribution to the energy of the YM term $\text{Tr}F^2$ in Eq. (1) also vanishes, consistently with the Derrick scaling requirement, and that indeed the YM potential becomes a *pure-gauge* in this limit. Thus the only contribution comes from the $\text{Tr}D\Phi^2$ term in Eq. (1), which in this case reduces to $\text{Tr}\partial\Phi^2$ of the scale invariant $O(3)$ sigma model on \mathbb{R}^2 . Our non-Abelian vortices in this limit are described by the radially symmetric vorticity- n subset of the non-interacting *self-dual* Belavin–Polyakov ferromagnetic vortices [20].

The effect of non-Abelianness on YMH solutions affects not only the energy values, which become lower for non-Abelian solutions, but also to the way the energy is distributed throughout space. Both for Abelian and non-Abelian configurations, solutions are radial for $n = 1$ (their energy density having the global maximum at the origin) and circular for $n > 1$ (their energy density hav-

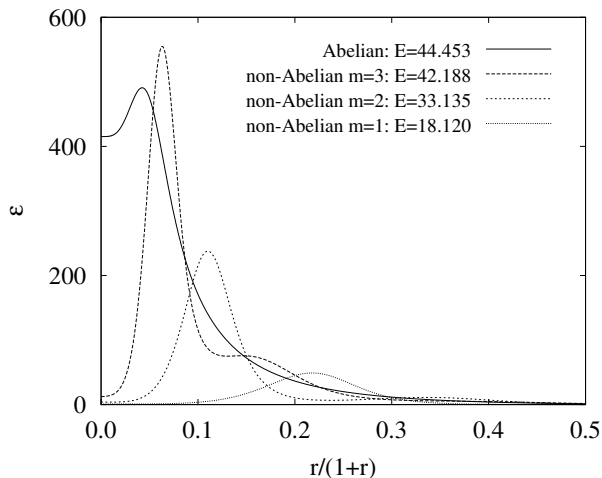


FIG. 4: Energy density for YMH solutions with $n = 3$ and $\lambda = 20.0$.

ing the global maximum at a finite non-vanishing value of r). For ring-shaped configurations ($n > 1$), as the solutions are more non-Abelian (lower values of m) the energy density profile spreads: the maximum is moved to higher values of r and its height decreases. In addition, the value of the energy density at the origin tends to zero, the profile becoming more and more ring-like. This result is demonstrated in Fig. 4 where the energy density

profiles of YMH solutions with $n = 3$ and $\lambda = 20.0$ are shown.

Conclusions

As a final comment on the possible physical status of our solutions, we emphasise that the model on \mathbb{R}^2 employed here is precisely that which supports monopoles on \mathbb{R}^3 . Interestingly, this YMH model on \mathbb{R}^3 supports also monopole-antimonopole (MA) solutions, constructed in [25]. This describes a consistent picture where our vortices are candidates for flux tubes starting and ending on monopoles of opposite polarities. Our results are qualitatively consistent with the picture in [25]. In particular for vorticities $n \geq 3$, the energy density distribution in the MA configuration presents a ring shaped density situated on the symmetry plane (the \mathbb{R}^2 plane where our vortices exist) much like the circles in Fig. 4.

We conclude by noting that the vortices constructed are genuinely non-Abelian, but are not endowed with a topological lower bound. That leads us to expect that these non-Abelian solutions are unstable for finite values of λ , even though the limiting solutions, namely the Belavin–Polyakov vortices for $\lambda \rightarrow \infty$ are stable.

Acknowledgement

We thank Jurgen Burzlaff, Eugen Radu and Valery Rubakov for helpful discussions. This work is supported in part by Science Foundation Ireland (SFI) project RFP07-330PHY, and, by Ministerio de Ciencia e Innovación of Spain projects FIS2006-12783-C03-02, and FIS2009-10614.

-
- [1] J. L. Gervais and A. Neveu, Phys. Rept. **23**, 237 (1976).
 - [2] H. B. Nielsen and P. Olesen, Nucl. Phys. B **61**, 45 (1973).
 - [3] H. J. de Vega, Phys. Rev. D **18**, 2932 (1978).
 - [4] H. J. de Vega and F. A. Schaposnik, Phys. Rev. D **34**, 3206 (1986).
 - [5] P. Suranyi, Phys. Lett. B **481**, 136 (2000) [arXiv:hep-lat/9912023].
 - [6] F. A. Schaposnik and P. Suranyi, Phys. Rev. D **62**, 125002 (2000) [arXiv:hep-th/0005109].
 - [7] M. A. C. Kneipp and P. Brockill, Phys. Rev. D **64**, 125012 (2001) [arXiv:hep-th/0104171].
 - [8] K. Konishi and L. Spanu, Int. J. Mod. Phys. A **18**, 249 (2003) [arXiv:hep-th/0106175].
 - [9] A. Marshakov and A. Yung, Nucl. Phys. B **647**, 3 (2002) [arXiv:hep-th/0202172].
 - [10] A. Hanany and D. Tong, JHEP **0307**, 037 (2003) [arXiv:hep-th/0306150].
 - [11] R. Auzzi, S. Bolognesi, J. Evslin, K. Konishi and A. Yung, Nucl. Phys. B **673**, 187 (2003) [arXiv:hep-th/0307287].
 - [12] M. Eto, Y. Isozumi, M. Nitta, K. Ohashi and N. Sakai, Phys. Rev. Lett. **96** (2006) 161601 [arXiv:hep-th/0511088].
 - [13] M. Shifman and A. Yung, Rev. Mod. Phys. **79**, 1139 (2007) [arXiv:hep-th/0703267].
 - [14] M. Eto, Y. Isozumi, M. Nitta, K. Ohashi and N. Sakai, J. Phys. A **39** (2006) R315 [arXiv:hep-th/0602170].
 - [15] T. W. B. Kibble, Commun. Math. Phys. **64**, 73 (1978).
 - [16] M. B. Hindmarsh and T. W. B. Kibble, Rept. Prog. Phys. **58**, 477 (1995) [arXiv:hep-ph/9411342].
 - [17] M. S. Volkov, Phys. Lett. B **644**, 203 (2007) [arXiv:hep-th/0609112].
 - [18] B. Julia and A. Zee, Phys. Rev. D **11**, 2227 (1975).
 - [19] J. Spruck and Y. Yang, arXiv:0810.1076 [hep-th].
 - [20] A. M. Polyakov and A. A. Belavin, JETP Lett. **22** (1975) 245 [Pisma Zh. Eksp. Teor. Fiz. **22** (1975) 503].
 - [21] F. Navarro-Lerida, E. Radu and D. H. Tchrakian, Phys. Rev. D **79**, 065036 (2009) arXiv: 0811.3524 [hep-th].
 - [22] J. Ambjorn and V. A. Rubakov, Nucl. Phys. B **256** (1985) 434.
 - [23] Y. Brihaye and J. Kunz, Phys. Rev. D **47** (1993) 4789.
 - [24] L. G. Yaffe, Phys. Rev. D **40** (1989) 3463.
 - [25] B. Kleihaus, J. Kunz and Y. Shnir, Phys. Rev. D **70**, 065010 (2004) [arXiv:hep-th/0405169].
 - [26] This mathematical phenomenon is familiar from the Weinberg–Salam (WS) model on \mathbb{R}^3 . There, when the Higgs mass (λ here) goes to infinity, the Higgs potential becomes the constraint equation for the 4 real components parametrising the complex doublet Higgs. This results in the $SU(2)$ (right or left) gauged Skyrme field supporting techniskyrmions [22], which then coincide with some sphalerons [23, 24] of the WS model.